Response Kinetics of Tethered *Rhodobacter sphaeroides* to Changes in Light Intensity

Richard M. Berry and Judith P. Armitage
Department of Biochemistry, University of Oxford, South Parks Road, Oxford OX1 3QU, United Kingdom

ABSTRACT *Rhodobacter sphaeroides* can swim toward a wide range of attractants (a process known as taxis), propelled by a single rotating flagellum. The reversals of motor direction that cause tumbles in *Eschericia coli* taxis are replaced by brief motor stops, and taxis is controlled by a complex sensory system with multiple homologues of the *E. coli* sensory proteins. We tethered photosynthetically grown cells of *R. sphaeroides* by their flagella and measured the response of the flagellar motor to changes in light intensity. The unstimulated bias (probability of not being stopped) was significantly larger than the bias of tethered *E. coli* but similar to the probability of not tumbling in swimming *E. coli*. Otherwise, the step and impulse responses were the same as those of tethered *E. coli* to chemical attractants. This indicates that the single motor and multiple sensory signaling pathways in *R. sphaeroides* generate the same swimming response as several motors and a single pathway in *E. coli*, and that the response of the single motor is directly observable in the swimming pattern. Photo-responses were larger in the presence of cyanide or the uncoupler carbonyl cyanide 4-trifluoromethoxyphenylhydrazone (FCCP), consistent with the photo-response being detected via changes in the rate of electron transport.

INTRODUCTION

The response of *Escherichia coli* to changes in the concentration of attractants such as aspartate has been well characterized. Swimming cells alternate between runs, in which several flagella form a rotating bundle that propels the cell, and tumbles, in which the bundle flies apart and the cell jiggles about on the spot (Berg and Brown, 1972). Runs are prolonged if the concentration of attractant in the vicinity of a cell is increasing with time, allowing cells to swim up gradients of attractant concentration (Brown and Berg, 1974). By tethering single flagellar filaments to glass coverslips and observing the resulting rotation of the cell body, the rotation of individual flagellar motors can be measured (Silverman and Simon, 1974). Motors alternate between counterclockwise (CCW) and clockwise (CW) rotation; runs are associated with CCW rotation, tumbles with CW. In response to step increases in attractant concentration, the bias (probability of rotating CCW) in tethered cells increases for a few seconds before returning to its original value (i.e., adapting to the new concentration; Block et al., 1982). The responses of motors of tethered cells can be understood in terms of the impulse response. In response to a very short-lived increase in concentration (an impulse), the bias increases for about 1 s, and then decreases for another 3 s before returning to baseline. The response to other changes in concentration can be derived from the convolution of the impulse response and the concentration change, indicating that bias is a linear function for small chemical stimuli in *E. coli* (Block et al., 1983; Segall et al., 1986).

The results above apply to sudden changes in concentrations on the order of 1 μM, or to steady concentration changes on the order of 1 μM/s (against a similar background concentration), which are of the magnitude that a swimming bacterium might encounter in its natural environment. In experiments where sudden, large concentration changes are imposed ($\sim$1 mM), the response saturates, and adaptation takes minutes rather than seconds (Berg and Tedesco, 1975). These saturating responses are easy to induce and to measure, and in mutagenesis studies they are useful indicators of the presence or absence of a response to a particular stimulus, or of the sign of a response. However, taxis in swimming bacteria necessarily occurs on a timescale of several seconds (Berg, 1988; Berg and Purcell, 1977). Studies of the physical nature of taxis itself and the subtler effects of mutations upon the sensory system require observation of the faster, nonsaturating responses that are seen to smaller stimuli.

Unlike *E. coli*, in which many flagella come together into a bundle to propel a swimming cell, *Rhodobacter sphaeroides* swims with a single subpolar flagellum. The flagellar motor rotates in only one direction, stopping briefly at random times (Armitage and Macnab, 1987; Armitage et al., 1999). During these stops the orientation of the cell changes rapidly and randomly, in much the same way as when *E. coli* motors switch to CW rotation to induce a tumble. *R. sphaeroides* is capable of taxis to a wide range of attractants including metabolites, light, and electron acceptors. When single cells are observed, either swimming or tethered, the bias (defined as the probability of the flagellar motor running rather than stopping) increases in response to large attractant stimuli and decreases in response to large repellent stimuli (Poole and Armitage, 1988). Thus, it appears

Received for publication 15 July 1999 and in final form 19 December 1999.

Dr. Berry's current address: The Randall Institute, King's College London, 26–29 Drury Lane, London WC2B 5RL, UK. Tel.: 0171 465 5377; Fax: 0171 497 9078; E-mail: richard.berry@kcl.ac.uk.

Address reprint requests to Judith P. Armitage, Department of Biochemistry, University of Oxford, South Parks Road, Oxford OX1 3QU, UK. Tel.: 01865 275299; Fax: 01865 275297; E-mail: armitage@bioch.ox.ac.uk.

0006-3495/00/03/1207/09 $2.00

that motor stopping in *R. sphaeroides* is analogous to tumbling in *E. coli.* The dominant response appears to be to repellent stimuli (reductions in attractant concentration), with only a small response seen to attractant stimuli (increases in attractant concentration). As both species of bacteria are approximately the same size and swim at similar speeds, they face the same physical constraints upon chemotaxis. That is to say, they can swim in a given direction for only a few seconds before being disoriented by Brownian motion, and size constraints mean that they sense temporal changes in their environment rather than spatial gradients (but see Dusenbery, 1998, for discussion). Because of these constraints, the responses of *R. sphaeroides* to physiologically relevant small stimuli might be expected to be similar to those of *E. coli*: adaptation in a few seconds to step changes, and an impulse response with an initial phase of the same sign as the stimulus, and a subsequent phase of the opposite sign.

Responses of *R. sphaeroides* to chemicals and light in the saturating, large-stimulus regime, measured over the course of several minutes (Gauden and Armitage, 1995; Packer et al., 1996), are similar to the saturating chemo-responses of *E. coli*. Here we show that the responses of tethered *R. sphaeroides* to light are also similar to the chemo-responses of *E. coli* in the subsaturating, small-stimulus regime. This indicates that both species use the same strategy of abrupt changes of direction controlled by temporal comparisons of their changing environment over the course of a few seconds. In *E. coli*, runs and tumbles are related in a complicated and imperfectly understood way to periods of CCW and CW rotation, whereas in *R. sphaeroides* runs and tumbles in swimming cells are the direct result of runs and stops in the single flagellar motor, suggesting that it may be a good species in which to study motor control in free-swimming cells.

The two species differ in what they can sense and in the complexity of the sensory pathway. *E. coli* has four membrane-spanning chemosensory transducers and one sensing changes in electron transport (Armitage, 1999). *R. sphaeroides* has at least 12 sensors located both in the membrane and in clusters in the cytoplasm; these latter may be involved in sensing the metabolic state of the cell (Armitage and Schmitt, 1997). Unlike *E. coli*, several attractants require transport and partial metabolism to be sensed (Ingham and Armitage, 1987; Jeziore-Sassoon et al., 1998; Poole and Armitage, 1989; Poole et al., 1993). Sensory signals in *E. coli* are processed and transmitted to the motors by a cytoplasmic phosphorelay pathway encoded by the genes *cheA*, *cheW*, *cheY*, *cheR*, and *cheB*. In *R. sphaeroides* there are several homologues of these genes, and the signal is transmitted through one of at least two phosphorelay pathways to the single motor (Hamblin et al., 1997; Armitage and Schmitt, 1997). Large-stimulus responses to oxygen and light are generated via changes in the rate of electron transport in the cell, signaling through one of the cytoplasmic pathways and probably involving a receptor (Romagnoli and Armitage, 1999; Grishanin et al., 1997; Gauden and Armitage, 1995). To confirm this result in the small-stimulus regime, we measured the effect on the photo-response of inhibitors which alter the rate of photosynthetic electron transport. Cyanide or small concentrations of the uncoupler carbonyl cyanide 4-trifluoromethoxyphenylhydrazone (FCCP), both of which are expected to cause up-regulation of photosynthetic electron transport, increased the size of responses to changes in light intensity. This provides further support for the hypothesis that behavioral responses are generated via changes in the rate of electron transport.

MATERIALS AND METHODS

Cell growth

R. sphaeroides strain WS8 was grown anaerobically in succinate medium (Harrison et al., 1994) at 30°C under bright light (wavelength range 400–800 nm, incident intensity 114 Wm^{-2}) in a flat glass growth chamber ~2 mm thick. Under these conditions, the doubling time was approximately 160 min and the exponential phase of growth lasted for 500 min, or three doublings. Cells were harvested after two doublings in exponential phase (~320 min), at which time the light intensity at the side farthest from the light source was reduced by a factor of about 2 from its original value and from the value at the side closest to the light source. Reducing this inhomogeneity by illuminating the chamber from both sides did not produce any noticeable change in the appearance or behavior of the cells.

Tethering

Cell cultures were taken from the light and immediately mixed with an equal volume of HEPES buffer (10 mM Na N-2-hydroxyethylpiperazine-N′-2-ethanesulphonic acid, pH 7.2), containing 100 μg/ml chloramphenicol to arrest protein synthesis. Cells were then washed twice in HEPES + 50 μg/ml chloramphenicol before tethering with anti-filament antibody in optically flat capillaries (Camlabs, Cambridge, UK) coated with the hydrophobic agent Sigmacote (Sigma-Aldrich, Poole, UK).

Data collection and analysis

Tethered cells were observed at high magnification in a light microscope (Fig. 1). To measure rotation rates, a phase-contrast image formed in light of wavelengths $\lambda > 950$ nm (beyond the range absorbed by the photosynthetic pigments) was projected onto the face of a quadrant photodiode (PIN-SPOT 4DMI, UDT Sensors, Inc., Hawthorne, CA) and the diode outputs recorded. Light at these wavelengths and the intensity used (200 Wm^{-2}) did not energize flagellar rotation. The image of a tethered cell was aligned such that the center of rotation coincided with the center of the quadrant photodiode (Fig. 2 *a*). Currents from the four quadrants, labeled a-d, were sampled at 128 Hz and the signals X and Y were calculated as indicated (Fig. 2 *b*). Envelopes were fitted to the extremes in X and Y to allow for drift (Fig. 2 *c*), and these signals were converted into $\cos\theta$ and $\sin\theta$, respectively (where θ is the angle of the cell body) by mapping the positive and negative envelopes to -1 and $+1$. θ was calculated as arctan(Y/X), and groups of four consecutive angles were averaged, reducing the sampling frequency to 32 Hz, before calculating the speed of rotation as $1/2\pi$ ($d\theta/dt$; Fig. 2 *d*).

Photo-stimulus

A second light source (λ between 500 and ~820 nm) was used to energize photosynthetic electron transport in the cells (Fig. 1). At 270 Wm^{-2}, the

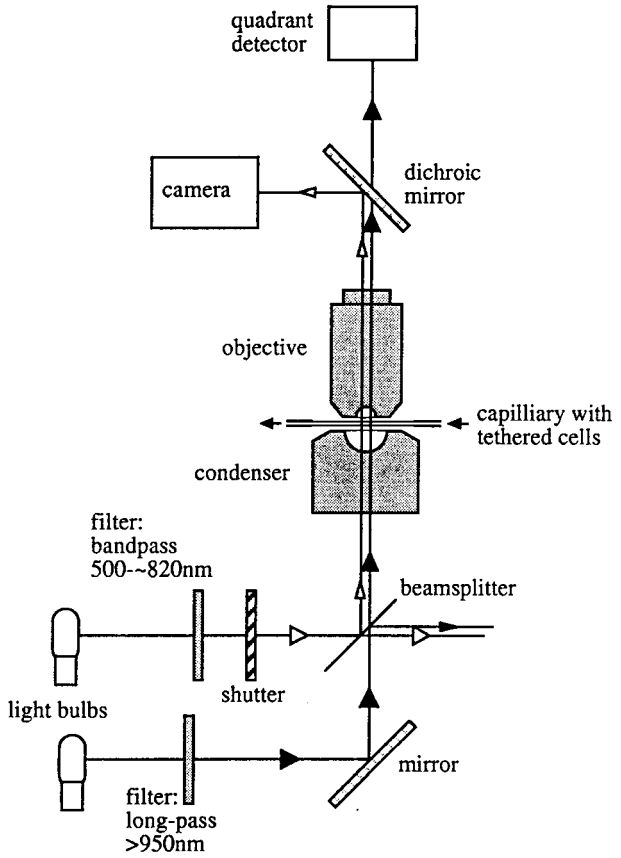

FIGURE 1 Photosynthetically grown R. sphaeroides were tethered in optically flat capillaries using anti-filament antibodies and observed at high magnification in a light microscope. To measure rotation rates, a phase-contrast image formed in light of wavelengths >950 nm was projected onto the face of a quadrant photodiode, and the diode outputs recorded by computer. A second light source (wavelength between 500 and ~820 nm) was used to energize photosynthetic electron transport in these cells. A shutter under computer control was used to block the energizing light for different lengths of time and the resulting changes in rotation were observed.

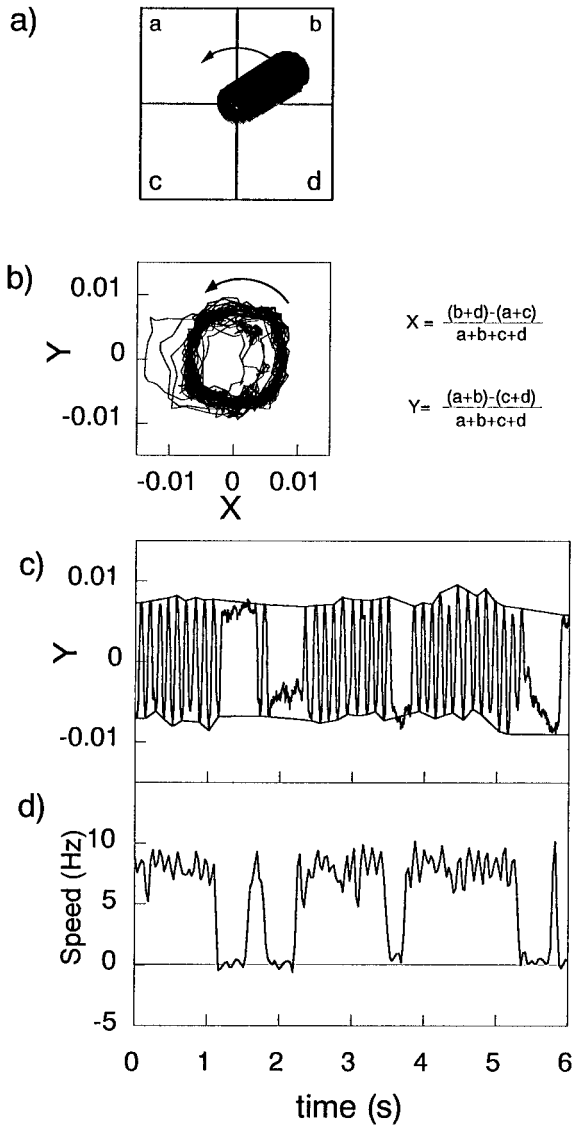

FIGURE 2 (*a*) An image of a tethered cell was aligned such that the center of rotation coincided with the center of the quadrant photodiode. (*b*) Currents from the 4 quadrants (labeled a-d) were recorded by computer and the signals X and Y were calculated as indicated. (*c*) Envelopes were fitted to the extremes in X and Y to correct for drift and these signals were converted into $\cos\theta$ and $\sin\theta$ respectively (where θ is the angle of the cell body) by mapping the positive and negative envelopes to -1 and $+1$. θ was calculated as arctan(Y/X), and the speed of rotation as $1/2\pi\,(d\theta/dt)$. (*d*) A typical record of speed versus time in light of constant intensity, characterized by sudden switches between rotating and stopped states at random times.

intensity of this light was more than adequate to saturate photosynthetic electron transport. Flagellar motors rotated at full speed, indicating a normal protonmotive force driven by cyclic photosynthetic electron transport, when illuminated at 20 Wm^{-2} or above, even in the presence of 1 mM cyanide to block respiration and 5 μM DCCD (N,N′-dicyclohexyl carbodiimide) to prevent the maintenance of a protonmotive force by ATP hydrolysis. A home-made shutter under computer control was used to block the energizing light for different lengths of time, and the resulting changes in rotation were observed.

Photo-responses

In order to measure a photo-response, the energizing light was repeatedly shuttered for a fixed time and multiple records of cell speed as a function of time from the closing of the shutter were obtained. These records were aligned, and two alternative measures of bias (the probability that a cell is rotating) were obtained. The first measure of bias was simply the fraction of records in which the cell was rotating at a given time from the closing of the shutter. "Rotating" was defined by a speed above a threshold equal to half the modal running speed, which in turn is defined as the most common speed in all of the records put together. The second measure of bias was the average speed over all records at a given time from the closing of the shutter, divided by the modal running speed. These two measures were very similar, and would be identical in an ideal data set where speeds switched between 0 and a fixed value, and all switches were detected. The latter method accounts for unresolved short intervals that would be ignored by the former.

Interval length distributions were calculated by measuring all intervals between crossings of the speed threshold that satisfied certain simple

criteria, designed to exclude errors due to an interval spanning the start or end of a record.

Altering electron transport rates

FCCP was added as a 0.1 mM solution in ethanol to final concentrations of 0.1 or 0.5 μM. At these concentrations the protonmotive force is retained close to its normal value, but electron transport is up-regulated to compensate for the FCCP-induced proton leakage (Armitage and Evans, 1985). Cyanide was added as a 1 M solution of NaCN in HEPES to a final concentration of 1 mM. At this concentration, respiratory electron transport is blocked and the protonmotive force is maintained by photosynthetic electron transport or, in the dark, by reversed F_1F_0-ATPase activity.

Computer simulation

Switching was modeled as a two-state process, with first-order rate constants for transitions into run or stop states given by

$$k_r = k_0 \exp\left(\frac{\Delta G(t)}{2kT}\right) \quad (1)$$

and

$$k_s = k_0 \exp\left(\frac{-\Delta G(t)}{2kT}\right) \quad (2)$$

respectively, where the time-varying free energy difference between the two states, $\Delta G(t)$, is specified by the user, k is Boltzmann's constant, and T the absolute temperature. The constant k_0 was calculated from the mean stop duration $\langle \tau_s \rangle = 0.27$ s (Fig. 3) and the resting bias $b^0 = 0.86$ (Fig. 5 *b*), via $k_0 = k_r^0 \exp(-\Delta G^0/2kT)$, where $k_r^0 = 1/\langle \tau_s \rangle$ is the rate constant for the transition from stop to run in unstimulated cells, and $\Delta G^0 = \ln(b^0/1 - b^0)$ is the free energy difference in unstimulated cells. Monte Carlo simulations were performed on a personal computer using the software package LabVIEW (National Instruments, Austin, TX). In each iteration, the time was advanced by $\Delta t = 0.001$ s, and the state was changed if a random number taken from an even distribution between 0 and 1 was less than Δt times the rate constant for transitions out of the previous state. The bias was obtained as the probability that the system was in the run state at a given time, averaged over an ensemble of 1000 simulations.

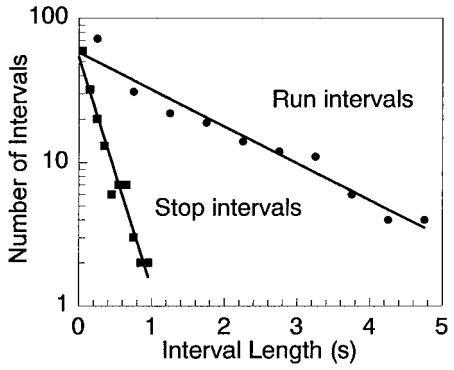

FIGURE 3 The distribution of intervals during which a cell was rotating (run intervals, *circles*) or stopped (stop intervals, *squares*). The cell was defined as running when its speed was greater than half the median speed for all data, and otherwise as stopped. The intervals are fitted as single exponentials with time constants of 0.27 and 1.69 s for stop and run intervals, respectively. Exponential distributions are consistent with a simple two-state model where switching occurs as the result of thermally driven transitions between run and stop states.

RESULTS

Unstimulated cells

Fig. 2, *a-c*, illustrates the method used to measure cell speed (see Materials and Methods), and Fig. 2 *d* shows a typical section from a record of speed versus time for a single wild-type *R. sphaeroides* in light of constant intensity. The behavior of the cell is characterized by sudden switches between rotating and stopped states at random times. When stopped, cells appeared to undergo free rotational Brownian motion. This was more evident in records where long stops were induced by repellent stimuli (removal of light) than it is in Fig. 2 *d*.

X and Y data were sampled at 128 Hz, and groups of four consecutive angles were averaged to give speeds at intervals of 1/32 s. Any stopped or rotating intervals shorter than this were not fully resolved by the system. For instance, a short stop at 0.3 s (Fig. 2 *c*) appears only as a transient slowing down in Fig. 2 *d*. Fig. 3 shows the interval length distribution for both run and stop intervals in one unstimulated cell. The distributions are good fits to single exponentials, as is the case in *E. coli*, indicating that switching of the flagellar motor is well described by a model with simple transitions between two states (Block et al., 1982; Turner et al., 1996; Scharf et al., 1998). The time constant for the stop interval distribution is 0.27 s. This means that one in nine stops will be shorter than the resolution time of 1/32 s, the probability of a stop lasting less than time T being given by $P = 1 - \exp(-T/0.27\text{ s})$, and will be missed by our measuring system. The video systems commonly used for measuring the rotation of tethered cells or the speed of swimming cells typically have even less temporal resolution, and will miss even more stops. For example, one stop in seven will be missed with a temporal resolution of 1/25 s, or one in three with a resolution time of 1/10 s.

Step Response

Fig. 4 shows the response of a *R. sphaeroides* cell to step changes in light intensity. The energizing light was alternately shuttered and transmitted in 20-s intervals. One period of this cycle is shown in Fig. 4 *a*. A typical response to this cycle is shown in Fig. 4 *b*. When the light was shuttered, at 20 s, the cell stopped within 1 s and returned to its normal pattern of stopping and rotating over the course of about 5 s. The histogram at the right is the distribution of all speeds observed in this experiment, with peaks at 0 and 12.5 Hz.

Fig. 4 *c* shows two alternative measures of bias (the probability that a cell is rotating) averaged over an ensemble of 20 consecutive identical cycles. The light line shows the fraction of cycles in which the cell was rotating at a given

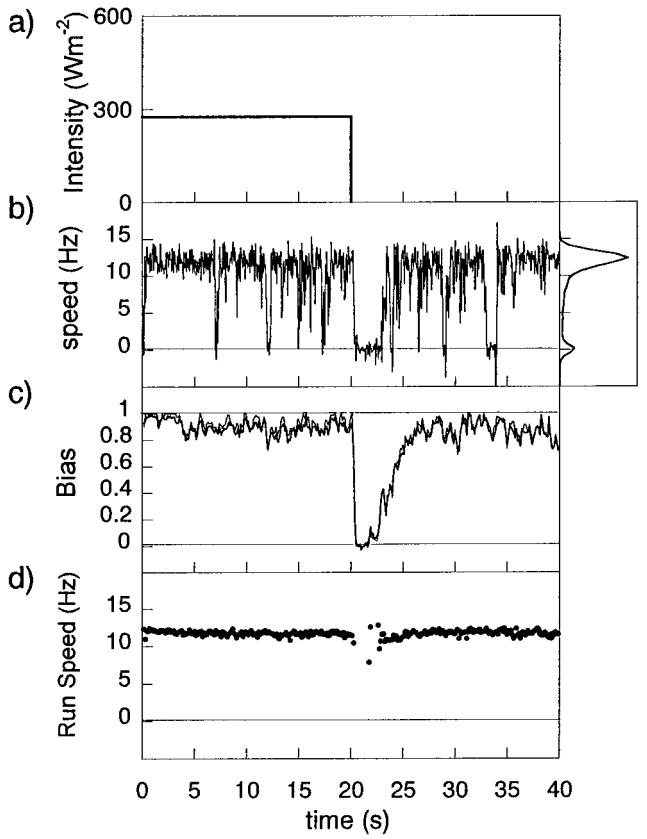

FIGURE 4 (*a*) To measure the response of cells to step changes in light intensity, the energizing light was alternately shuttered and transmitted in 20-s intervals. One period of this cycle is shown. (*b*) A typical response to the cycle in (*a*). When the light was shuttered, at 20 s, the cell stopped within 1 s and returned to its normal pattern of rotating and stopping over the course of about 5 s. The histogram at the right is the distribution of all speeds observed in this experiment, with peaks at 0 and 12.5 Hz corresponding to stopped and rotation states respectively. (*c*) Two alternative measures of bias, the probability that the cell is rotating, averaged over an ensemble of 20 consecutive identical cycles. The *light line* shows the fraction of cycles in which the cell was rotating at a given time in the cycle, and the *heavy line* shows the average speed over the ensemble divided by the modal run speed of 12.5 Hz. The two measures are very similar, but the latter accounts for unresolved short stop intervals that would be ignored by the former. In response to the step-down in light intensity, the cell always stopped within about 1 s and adapted back to its resting bias of 0.85 over the next 5 to 7 s. A response of similar duration and opposite sign is seen to the step-up in light at $t = 0$, although this is less clear because the resting bias is so close to 1. (*d*) The average speed of the cell when running. There is no evidence of photokinesis; the cell does not speed up when the light is stepped up, nor slow down when the light is stepped down.

time in the cycle, with rotating defined as a speed above 6.25 Hz. The heavy line shows the average speed at a given time in the cycle, divided by the modal speed of 12.5 Hz. These two methods give very similar results here, but the latter method accounts for unresolved short intervals that are ignored by the former, and for this reason is chosen as the more reliable measure of bias in the calculation of impulse responses.

The unstimulated or resting bias of this cell was about 0.85. In response to the step-down in light intensity, the cell always stopped within about 1 s, and adapted back to its resting bias over the next 5 to 7 s. A response of similar duration and opposite sign was seen to the step-up in light at $t = 0$, although this is less clear because the resting bias is so close to 1. Fig. 4 *d* shows the average speed of the cell when it was not stopped. There was no evidence of photokinesis, i.e., the running speed of the cell did not increase when the light was stepped up at $t = 0$, nor did it decrease when the light was stepped down at $t = 20$ s.

Impulse response

The response to a very short stimulus, or impulse response, is a fundamental measure of any system. One of its advantages is sensitivity. In typical chemotaxis experiments, millimolar step changes in attractant concentration saturate the cell responses for several minutes, whereas to be relevant to taxis under natural conditions, responses should occur on a timescale of several seconds. The step changes in light intensity shown in Fig. 4 also saturate the response, albeit for only a few seconds. For a more sensitive measure of photo-responses, the energizing light was shuttered for fractions of a second and the resulting changes in bias were observed.

Fig. 5 *a* shows the bias as a function of time after a brief (0.21 s) removal of energizing light (the impulse response) for a single cell. The dark period is marked by the small vertical lines just after $t = 0$, and bias was calculated using the second method described above for 51 identical impulses. The resting bias of approximately 0.8 is marked by the thin horizontal line. We chose repellent, or negative, stimuli (removal of light) rather than attractant stimuli (flashes of light in a dark background) because the high resting bias results in negative responses that are larger, and therefore easier to measure, than positive responses.

Fig. 5 *b* shows the average impulse response for five different cells. As in *E. coli*, the impulse response (to a negative stimulus) has an initial negative phase lasting about 1 s, and a subsequent, slightly longer positive phase (Block et al., 1982). There are two main differences between the responses of *E. coli* and *R. sphaeroides*. First, the average resting bias is ~0.85, compared to ~0.6 for tethered *E. coli*. This is similar to the probability of running versus tumbling in free-swimming *E. coli* (Berg and Brown, 1972). Second, the area under the second phase of the response is smaller than the area under the first phase. In *E. coli* these areas are equal, which is necessary for adaptation in the case where the response system is linear. Bias is, therefore, not a linear function of stimulus in *R. sphaeroides* photo-responses. This is not surprising given the high resting bias. In a two-state system the bias at equilibrium is related to the free energy difference between rotating and

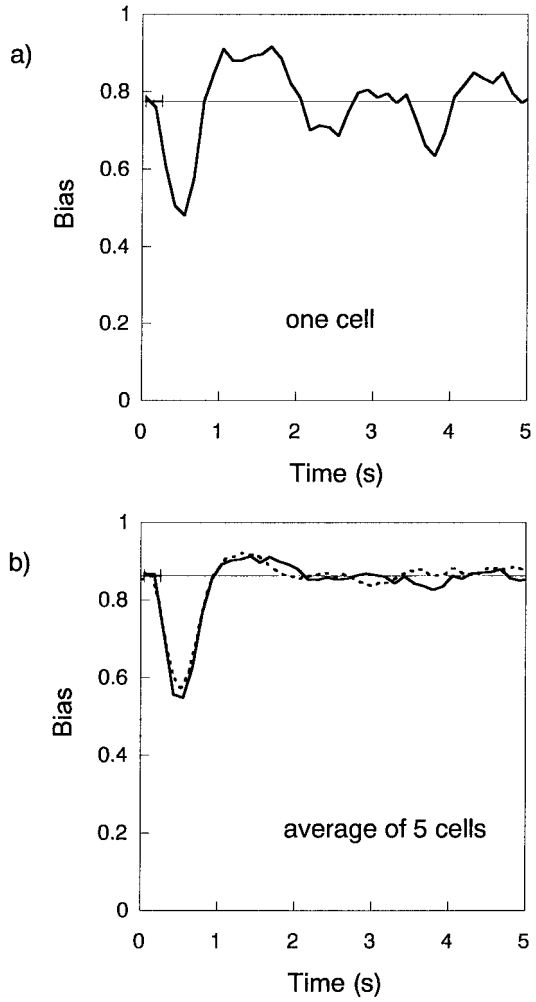

FIGURE 5 (*a*) The impulse response of a single tethered cell of *R. sphaeroides* in HEPES buffer. In response to a brief removal of the energizing light (for 0.21 s, the interval marked by the small vertical bars) the bias falls for about 1 s, returns and overshoots for a further second, and then falls back to its resting level marked by the horizontal line. (*b*) The average impulse response of 5 different cells (*solid line*). The impulse stimulus was presented to each cell between 40 and 60 times and the bias was calculated by the second method described in the legend to Fig. 4. The cell was allowed 15 s between impulses to ensure that it had returned fully to its resting condition. The *dotted line* shows the impulse response predicted by computer simulation (see text and Fig. 6 *b*).

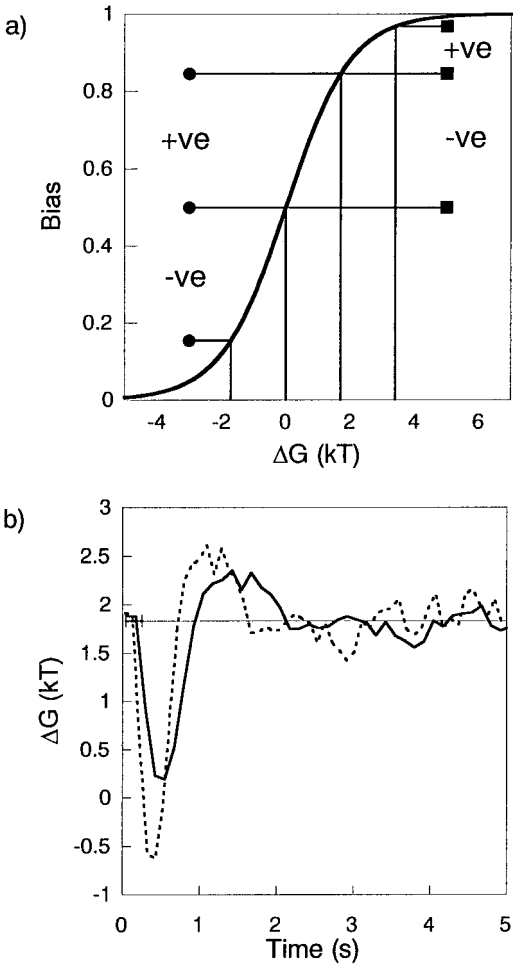

FIGURE 6 (*a*) The relationship between bias and the free energy difference between rotating and stopped states (ΔG) in a two-state model of motor switching. When ΔG is zero, the states have equal probability and the bias is 0.5. If a sensory stimulus leads to symmetrical changes in ΔG (shown by the *vertical lines* at an equal spacing of 1.7 *kT* in the figure, where k is Boltzmann's constant and T the absolute temperature), this produces symmetrical responses in bias when the starting bias is 0.5 (*circles*), but a much reduced positive (+) response when the starting bias is 0.85 (*squares*). (*b*) The impulse response of Fig. 5 *b* plotted as ΔG rather than as bias. The solid line shows equilibrium values of ΔG, calculated using Eq. 4. The *dotted line* shows the values that were used in a computer simulation to fit the measured bias (see Fig. 5 *b*). This compensates for the effect of the relationship between bias and ΔG illustrated in (*a*). Nonetheless, even in terms of ΔG the positive phase of the response is smaller than the negative.

stopped states, ΔG, by

$$bias = \frac{\exp(\Delta G/kT)}{1 + \exp(\Delta G/kT)} \quad (3)$$

where k is Boltzmann's constant and T the absolute temperature.

This function is plotted in Fig. 6 *a*. The sigmoidal shape of the curve means that the change in bias for a given change in ΔG will be largest at values of bias close to half, and much smaller at values of bias close to 0 or 1. The circles show the changes in bias caused by changing ΔG by plus or minus 1.7 *kT* from a starting bias of 0.5, and the squares show the results of the same changes in ΔG but with a starting bias of 0.85. With a starting bias of 0.5 (like *E. coli*), the changes in bias are large and symmetrical, and bias is an almost linear function of ΔG. With a starting bias of 0.85 (like *R. sphaeroides*), the positive change in bias is much smaller than the negative, and bias is far from being a linear function of ΔG.

Fig. 6 *b* shows the impulse response from Fig. 5 *b* plotted in terms of ΔG. The solid line shows ΔG calculated as

$$\Delta G_{eq} = \ln\left(\frac{bias}{1 - bias}\right) \quad (4)$$

This expression assumes that the switching process reaches equilibrium on a timescale that is fast compared with the impulse response, so that the experimentally measured bias is given by Eq. 3. However, the timescale of switching (see Fig. 3) is in fact on the same order as that of the impulse response. Calculation of ΔG from bias in this non-equilibrium case is not trivial. Therefore, to examine the relationship between ΔG and measured bias, we performed a Monte Carlo computer simulation of the switching process in which the time-varying rate constants for switching are derived from a user-specified time course for ΔG and the interval length data of Fig. 3 (see Materials and Methods). When the solid line in Fig. 6 *b* was used as the specified time course, the model predicted a bias response that was smaller and slower than the actual measured response. However, the model can be made to predict the measured bias response simply by rescaling the time course of ΔG. The dotted line in Fig. 6 *b* shows the rescaled time course, produced from the solid line by simply multiplying deviations of ΔG from its resting value by 1.5 and speeding up the time course by a factor of 1.3. The dotted line in Fig. 5 *b* shows the corresponding predicted bias, which agrees with the measured values to well within the limits of experimental error.

Presenting the impulse response as ΔG rather than as bias emphasizes the positive phase relative to the negative, but in Fig. 6 *b* the areas are still unequal. The calculated values of ΔG are very sensitive to errors in measured values of bias at these extreme biases, but nonetheless the data suggest that ΔG, like bias, is not a linear function of stimulus in *R. sphaeroides* photo-responses. This again is not unexpected. In the model of Scharf et al. (1998) for switching of the flagellar motor of *E. coli*, ΔG is a linear function of the number of molecules of phosphorylated CheY (CheY-P) that are bound to the motor. This number is a saturating function of CheY-P concentration, which in turn depends in an unknown way upon the stimulus. Given all these factors, perhaps it is more surprising that bias is a linear function of stimulus in the response of *E. coli* to chemicals than that it is not in the response of *R. sphaeroides* to light.

Effects of inhibitors on impulse responses

Fig. 7 shows the size of impulse responses as a function of the stimulus size in HEPES buffer, buffer plus uncoupler (FCCP, 0.1 μM), and buffer plus cyanide (CN, 1 mM). Stimulus size is defined as the time for which the shutter was closed, and response size is defined as the sum of the areas of the two phases of the impulse response, as shown in Fig. 5 *b*. The approximate linearity between response and stimulus is to be expected if the stimuli are not saturating and are effectively impulse stimuli, that is to say, of shorter duration than any features in the response. This is true for 0.1-s and 0.2-s stimuli, less so for 0.4-s stimuli.

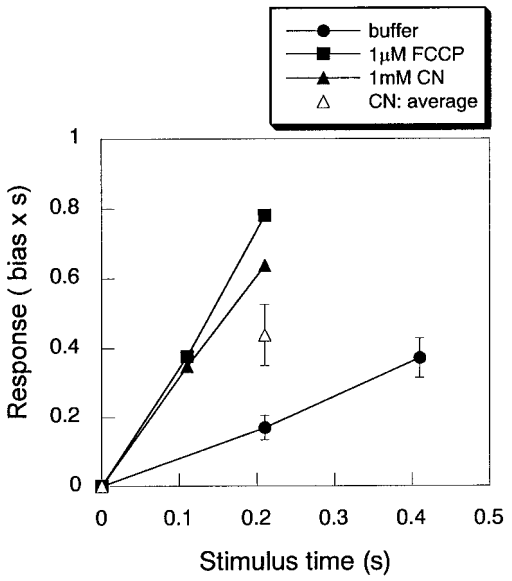

FIGURE 7 The magnitude of the impulse response as a function of stimulus size in HEPES buffer (*circles*), buffer plus 1 μM FCCP (*squares*) and buffer plus 1 mM cyanide (*triangles*). Response size is the sum of the areas of the two phases of the impulse response as shown in Fig. 5 *a*, stimulus size is the time for which the shutter was closed. Cyanide and low concentrations of FCCP both increase the size of the response to a given stimulus. This is consistent with the hypothesis that the photo-response is generated via changes in the rate of electron transport. Both FCCP and cyanide are expected to increase the rate of photosynthetic electron transport, and therefore also to increase the changes in this rate when the light is removed. Responses in buffer alone (*circles*) are shown as the mean and standard error of data from 5 cells. The *open triangle* for cyanide shows the mean and standard error of data from 4 cells, the *filled triangles and squares* show data from single cells with cyanide and FCCP, respectively.

In the presence of FCCP or cyanide, the resting bias, shape, and time course of the impulse response are similar to those in HEPES buffer alone. The magnitude of response for a given stimulus, however, is several times greater when either FCCP or CN is present. At the concentrations used, both FCCP and CN are expected to increase the rate of photosynthetic electron transport to maintain the protonmotive force: FCCP by allowing protons to leak across the membrane, CN by blocking respiratory electron transport. The experiments were not conducted under strictly anaerobic conditions and there would be electron transport to a terminal oxidase in addition to photosynthetic flow, as reported by Grishanin et al. (1997). Previous work has shown a repellent response in *R. sphaeroides* to the removal of low concentrations of FCCP, and an attractant response to its addition (Gauden and Armitage, 1995; the attractant response is visible in Fig. 6 of that paper but is not discussed).

A similar attractant response to the addition of FCCP was seen here (data not shown), with an almost total suppression of stopping for several minutes after the addition of FCCP. It has also been observed that saturating negative responses to prolonged removal of light are larger in the presence of low concentrations of FCCP (Grishanin et al., 1997). These data lend support to the hypothesis that *R. sphaeroides* responds to light, oxygen, and a variety of metabolic effectors by detecting changes in the rate of electron transport. Cyanide or low concentrations of FCCP both probably increase the rate of photosynthetic electron transport under the conditions used here, and therefore also increase the changes in this rate upon removal of light. This leads to an increase in the negative photo-response.

DISCUSSION

Our main finding is that the responses of *R. sphaeroides* to small photo-stimuli are essentially the same as those of *E. coli* to small chemical stimuli. Motors adapt to step changes after about 5 s, and the impulse response consists of an initial phase of the same sign as the stimulus, lasting about 1 s, and a subsequent, slightly longer, phase of the opposite sign. The only significant difference is that the resting bias of *R. sphaeroides* (tethered by its single motor) is close to 1, more like the run/tumble bias of *E. coli* swimming with a bundle of several flagella than the CCW/CW bias of *E. coli* tethered by a single motor. The high resting bias in tethered *R. sphaeroides* makes positive responses harder to observe in this species. With a resting bias of 0.85, the maximum possible positive change is only 0.15, close to the limit of detection in earlier experiments, which led to the belief that *R. sphaeroides* responds to negative but not to positive stimuli. Here we show, however, that positive responses to positive stimuli, although harder to measure than negative responses, are nonetheless present in *R. sphaeroides*.

In this work we have measured the rotation of tethered *R. sphaeroides* cells with greater accuracy and temporal resolution than in previous studies. Our data indicate that the phenomenon of chemokinesis (Brown et al., 1993; Packer and Armitage, 1994), in which motors appear to speed up in response to the addition of high concentrations of chemical attractants, may be due to the suppression of stops that are too short to be detected by the video measuring system, rather than to actual increases in the running speed of the motor. The predominance of short-lived stops in *R. sphaeroides* means that many stops will be too short to be detected, and will appear instead as a reduction in the average speed of the motor. The prolonged suppression of stops that occurs when high concentrations of attractants are added will remove this reduction in speed and appear as a speed increase. Transient increases in swimming speed in response to increases in light intensity (Romagnoli et al., 1999; Armitage et al., 1999) may also be explained as the suppression of unresolved stops, although actual increases in swimming speed are not ruled out by our results. With this in mind, our results are consistent with those of Romagnoli et al. (1999), in both the presence and absence of FCCP.

Although *E. coli* and *R. sphaeroides* are very similar in terms of behavioral responses themselves, they differ in the stimuli they respond to and in the nature of their sensory systems. The response of *E. coli* to aspartate begins with a change in the fraction of transmembrane aspartate receptors (Tar) that have aspartate bound, and it is usually assumed that this fraction comes rapidly to equilibrium when the concentration is changed (Brown and Berg, 1974). In the photo-response of *R. sphaeroides*, presumably, the place of aspartate is taken by the oxidized or reduced form of some unspecified component(s) of the electron transport chain (call it or them Q), and that of Tar by some unspecified receptor. The identities of Q and of the receptor remain to be determined. It also remains to be seen whether Q simply binds to the receptor or generates a signal by electron transfer to the receptor, as is probably the case in Aer (Taylor and Zhulin, 1998). The other major difference between the two species is that *R. sphaeroides* has multiple homologous copies of the sensory system genes. To date there are 3 *cheA*s, 4 *cheYs,* 3 *cheWs*, 2 *cheR*s and 1 *cheB* (Armitage and Schmitt, 1997). Why does *R. sphaeroides* have so many taxis genes? Perhaps some of them are expressed only in response to specific conditions, encountered in the wild but not as yet in laboratory experiments. The task ahead is to understand how the multitude of chemotaxis genes in *R. sphaeroides* is arranged into different sensory pathways, what these pathways sense, and how they are integrated.

The results shown here indicate that whatever the stimulus or the sensory pathway, the resulting behavioral response is likely to be very similar for most species of this size that swim at similar speeds through liquid media propelled by rotating flagella. Presumably the high bias of the *R. sphaeroides* motor evolved to optimize taxis based on swimming with a single flagellum. The lower bias of the *E. coli* motor, on the other hand, reflects the need to average the responses of multiple motors to produce the same kinetics in swimming cells. *R. sphaeroides* may be an ideal species for investigating tactic responses under natural conditions, as the kinetics of the motor are directly reflected in free-swimming behavior. Furthermore, the possibility of using light as a stimulus should make it experimentally easier to apply well controlled and rapid stimuli.

This work was supported by the Wellcome Trust.

REFERENCES

Armitage, J. P. 1999. Bacterial tactic responses. *Adv. Microb. Physiol.* 41:229–289.

Armitage, J. P., and M. C. W. Evans. 1985. Control of the protonmotive force in *Rhodopseudomonas sphaeroides* in the light and dark and its

effect on the initiation of flagellar rotation. *Biochim. Biophys. Acta.* 1:42–55.

Armitage, J. P., and R. M. Macnab. 1987. Unidirectional intermittent rotation of the flagellum of *Rhodobacter sphaeroides*. *J. Bacteriol.* 169:514–518.

Armitage, J. P., and R. Schmitt. 1997. Bacterial chemotaxis: *Rhodobacter sphaeroides* and *Sinorhizobium meliloti*-variations on a theme. *Microbiol.* 143:3671–3682.

Armitage, J. P., T. P. Pitta, M. A-S. Vigeant, H. L. Packer, and R. M. Ford. 1999. Transformations in flagellar structure of *Rhodobacter sphaeroides* and possible relationship to changes in swimming speed. *J. Bacteriol.* 181: In press.

Berg, H. C. 1988. A physicist looks at bacterial chemotaxis. *Cold Spring Harbour Symp. Quant. Biol.* 53:1–10.

Berg, H. C., and D. A. Brown. 1972. Chemotaxis in *Escherichia coli* analysed by three-dimensional tracking. *Nature.* 239:500–504.

Berg, H. C., and E. M. Purcell. 1977. Physics of chemoreception. *Biophys. J.* 20:193–219.

Berg, H. C., and P. M. Tedesco. 1975. Transient response to chemotactic stimuli in *Escherichia coli*. *Proc. Natl. Acad. Sci. USA.* 72:3235–3239.

Brown D. A., and H. C. Berg. 1974. Temporal stimulation of chemotaxis in *Escherichia coli*. *Proc. Natl. Acad. Sci. USA.* 71:1388–1392.

Block, S. M., J. E. Segall, and H. C. Berg. 1982. Impulse responses in bacterial chemotaxis. *Cell.* 31:215–226.

Block, S. M., J. E. Segall, and H. C. Berg. 1983. Adaptation kinetics in bacterial chemotaxis. *J. Bacteriol.* 154:312–323.

Brown, S., P. S. Poole, W. Jeziorska, and J. P. Armitage. 1993. Chemokinesis in Rhodobacter sphaeroides is the result of a long-term increase in the rate of flagellar rotation. *Biochim. Biophys. Acta.* 1141:309–312.

Dusenbery, D. B. 1998. Spatial sensing of stimulus gradients can be superior to temporal sensing for free-swimming bacteria. *Biophys. J.* 74:2272–2277.

Gauden, D. E., and J. P. Armitage. 1995. Electron transport-dependent taxis in Rhodobacter sphaeroides. *J. Bacteriol.* 177:5853–5859.

Grishanin, R. N., D. E. Gauden, and J. P. Armitage. 1997. Photoresponses in Rhodobacter sphaeroides: role of photosynthetic electron transport. *J. Bacteriol.* 179:24–30.

Hamblin, P. A., B. A. Maguire, R. N. Grishanin, and J. P. Armitage. 1997. Evidence for two chemosensory pathways in *Rhodobacter sphaeroides*. *Mol. Microbiol.* 26:1083–1096.

Harrison, D. M., H. L. Packer, and J. P. Armitage. 1994. Swimming speed and chemokinetic response of *Rhodobacter sphaeroides* investigated by natural manipulation of the membrane potential. *FEBS Lett.* 348:37–40.

Ingham, C. J., and J. P. Armitage. 1987. Involvement of transport in *Rhodobacter sphaeroides* chemotaxis. *J. Bacteriol.* 169:5801–5807.

Jeziore-Sassoon, Y., P. A. Hamblin, C. A. Bootle-Wilbraham, P. S. Poole, and J. P. Armitage. 1998. Metabolism is required for chemotaxis to sugars in *Rhodobacter sphaeroides*. *Microbiology.* 144:229–239.

Packer, H. L., and J. P. Armitage. 1994. The chemokinetic and chemotactic behavior of *Rhodobacter sphaeroides*: two independent responses. *J. Bacteriol.* 176:206–212.

Packer, H. L., D. E. Gauden, and J. P. Armitage. 1996. The behavioural response of anaerobic *Rhodobacter sphaeroides* to temporal stimuli. *Microbiology.* 142:593–599.

Poole, P. S., and J. P. Armitage. 1988. Motility response of *Rhodobacter sphaeroides* to chemotactic stimulation. *J. Bacteriol.* 170:5673–5679.

Poole, P. S., and J. P. Armitage. 1989. Role of metabolism in the chemotactic response of *Rhodobacter sphaeroides* to ammonia. *J. Bacteriol.* 171:2900–2902.

Poole, P. S., M. J. Smith, and J. P. Armitage. 1993. Chemotactic signalling in *Rhodobacter sphaeroides* requires metabolism of attractants. *J. Bacteriol.* 175:291–294.

Romagnoli, S., and J. P. Armitage. 1999. Roles of chemosensory pathways in transient changes in swimming speed of *Rhodobacter sphaeroides* induced by changes in photosynthetic electron transport. *J. Bacteriol.* 181:34–39.

Scharf, B. E., K. A. Fahrner, L. Turner, and H. C. Berg. 1998. Control of direction of flagellar rotation in bacterial chemotaxis. *Proc. Natl. Acad. Sci. USA.* 95:201–206.

Segall, J. E, S. M. Block, and H. C. Berg. 1986. Temporal comparisons in bacterial chemotaxis. *Proc. Natl. Acad. Sci. USA.* 83:8987–8991.

Silverman, M., and M. Simon. 1974. Flagellar rotation and the mechanism of bacterial motility. *Nature.* 249:73–74.

Taylor, B. L., and I. B. Zhulin. 1998. In search of higher energy: metabolism-dependent behaviour in bacteria. *Mol. Microbiol.* 28:683–690.

Turner, L., S. R. Caplan, and H. C. Berg. 1996. Temperature-induced switching of the bacterial flagellar motor. *Biophys. J.* 71:2227–2233.